HYPERMIX: A NEW TOOL FOR QUANTITATIVE EVALUATION OF ENDMEMBER IDENTIFICATION AND SPECTRAL UNMIXING TECHNIQUES

Luis-Ignacio Jiménez, Gabriel Martín and Antonio Plaza

Hyperspectral Computing Laboratory, Department of Technology of Computers and Communications, University of Extremadura, E-10003 Caceres, Spain.

ABSTRACT

In this paper, we present a new open source system for evaluating and inter-comparing new spectral unmixing applications. The proposed tool, called HyperMix, comprises several open source implementations of algorithms for endmember identification and spectral unmixing. The tool also includes a database of synthetic hyperspectral images (generated using fractals to simulate natural patterns) which can be used to evaluate the precision of the algorithms for endmember identification and abundance estimation which are already incorporated in the tool. The paper also presents an exhaustive inter-comparison of algorithms for endmember extraction and abundance estimation using the proposed tool.

***Index Terms*—** Hyperspectral imaging, endmember extraction, spectral unmixing, open-source tools.

1. INTRODUCTION

Hyperspectral imaging is a technique in remote sensing that collects hundreds of images, at different wavelength values, for the same area in the surface of the Earth [1]. For instance, the Airborne Visible Infra-Red Imaging Spectrometer (AVIRIS) instrument operated by NASA's Jet Propulsion Laboratory collects 224 spectral channels in the wavelength range from 40 to 250 nanometers using narrow spectral bands [2]. The new generation of satellite hyperspectral instruments improves this spectral resolution even more, providing very detailed spectral information about ground cover materials. However, the spatial resolution of hyperspectral imaging instruments is still in the range of several meters per pixel. As a result, the pixels collected by an imaging spectrometer are likely mixed in nature [3].

Spectral unmixing is a very important tool in remotely sensed hyperspectral data exploitation which aims at estimating the abundance of pure spectral components (called *endmembers*) in each mixed pixel [4]. During the past years, many algorithms and models have been developed for endmember identification and abundance estimation in remotely sensed hyperspectral images [5, 6], thus making spectral unmixing a hot topic in the hyperspectral imaging literature. However, the codes and implementations of these algorithms have not been available in open source format as of yet, and there is no clearly standardized data set for benchmarking the accuracy of spectral unmixing techniques.

In this paper, we present a first significant effort towards the adoption of a standardized and open source system for evaluating and inter-comparing new spectral unmixing applications. The proposed tool, called HyperMix, has been developed using the Orfeo Toolbox [1], an open source library of image processing algorithms. The tool comprises several open source implementations of algorithms for endmember identification and spectral unmixing. In addition, the tool also includes a database of synthetic hyperspectral images (generated using fractals to simulate natural patterns) which can be used to evaluate the precision of the algorithms for endmember identification and abundance estimation which are already incorporated in the tool. In this paper, we also present an exhaustive inter-comparison of algorithms for endmember extraction and abundance estimation using the considered tool, covering the most recent developments in the field and establishing a quantitative and comparative assesment in terms of algorithm precision and computational efficiency using both synthetic and real hyperspectral data sets.

2. THE HYPERMIX TOOL

The HyperMix tool is available online for public download and evaluation[2]. It comprises different algorithms that cover the standard hyperspectral unmixing chain, which is graphically illustrated by a flowchart in Fig. 1. The unmixing chain consists of three main parts: 1) dimensional reduction, 2) selection of pure spectral signatures or endmembers, and 3) estimation of the abundance of each endmember in each pixel of the scene. For illustrative purposes, Fig. 2 shows the visual appearence of the HyperMix tool, which has been developed

This work has been supported by the European Community's Marie Curie Research Training Networks Programme under contract MRTN-CT-2006-035927, Hyperspectral Imaging Network (HYPER-I-NET). Funding from the Spanish Ministry of Science and Innovation (CEOS-SPAIN project, reference AYA2011-29334-C02-02) is also gratefully acknowledged.

[1] http://orfeo-toolbox.org/otb

[2] http://www.hypercomp.es/hypermix

to address the full hyperspectral unmixing chain in Fig. 1. The following specific techniques are implemented for each part of the unmixing chain:

1. **Dimensional reduction**. For this purpose, the tool includes an open source implementation of principal component analysis (PCA) [7].

2. **Endmember selection**. For this purpose, the tool includes algorithms using spectral information: N-FINDR [8], orthogonal subspace projection (OSP) [9], vertex component analysis (VCA) [10] and also algorithms using both spatial and spectral information: automated morphological endmember extraction (AMEE) [11], spatial-spectral endmember extraction (SSEE) [12], and spatial pre-processing (SPP) [13].

3. **Abundance estimation**. For this purpose, the tool includes an unconstrained least-squares (ULS) abundance estimation approach [14] and also a fully constrained (FCLS) approach [15] which includes both non-negativity and sum-to-one constraints when estimating the abundance of endmembers in each pixel of a hyperspectral image.

3. USING HYPERMIX WITH SYNTHETIC HYPERSPECTRAL DATA

A database of 100×100-pixel synthetic hyperspectral scenes created using fractals to generate distinct spatial patterns has been included in the HyperMix tool to allow quantitative evaluation of spectral unmixing techniques using this tool. Fig. 2(a) shows an example of processing a synthetic hyperspectral image with HyperMix. The reason for using fractals is that several natural objects can be approximated by fractals to a certain degree, including clouds, mountain ranges, coastlines, vegetables, etc. thus providing a baseline for simulating spatial patterns often found in nature. The synthetic images are simulated from linear mixtures of a set of endmember signatures randomly selected from a spectral library compiled by the U.S. Geological Survey (USGS)[3] and made up of a total of 420 signatures. These images are further divided into a number of clusters using the k-means algorithm [16], where the number of clusters extracted from the five fractal images was always larger than the number of endmember signatures, fixed in our experiments to nine endmembers per scene. The abundance proportions in the regions associated to each cluster have been set so that pixels closer to the border of the region are more heavily mixed, while the pixels located at the center of the region are more spectrally pure in nature (the images does not contain any completely pure pixels, a situation often encountered in real-world analysis scenarios). Zero-mean Gaussian noise was added to the synthetic scenes in different signal to noise ratios (SNRs) –from 30:1 to 110:1– to simulate contributions from ambient and instrumental sources, following the procedure described in [9].

The metric used to compare the performance of endmember identification algorithms in this work is the spectral angle [3] between each extracted endmember and the set of available USGS ground-truth spectral signatures. The lowest the spectral angle, the better the results. Table 1 shows the average spectral angle scores (in degrees) between the reference USGS mineral spectra and their corresponding endmember pixels produced by several endmember extraction algorithms included in HyperMix, across the considered synthetic scenes. As shown by Table 1, the OSP and VCA (based on spectral information alone) generally provided the best result in the comparison, although the inclusion of spatial information through SPP helped improving the results in some particular cases.

4. USING HYPERMIX WITH REAL HYPERSPECTRAL DATA

We have also used the HyperMix tool to analyze the well-known AVIRIS Cuprite data set, available online in reflectance units[4] after atmospheric correction. This scene has been widely used to validate the performance of endmember identification algorithms. The portion used in experiments corresponds to a 350×350-pixel subset of the sector labeled as f970619t01p02_r02_sc03.a.rfl in the online data. The scene comprises 224 spectral bands between 0.4 and 2.5 μm, with full width at half maximum of 10 nm and spatial resolution of 20 meters per pixel. Prior to the analysis, several bands were removed due to water absorption and low SNR in those bands, leaving a total of 192 reflectance channels to be used in the experiments. Fig. 2(b) shows an example of processing the AVIRIS Cuprite image with HyperMix. The Cuprite site is well understood mineralogically [17], and has several exposed minerals of interest included in the USGS spectral library. A few selected spectra from the USGS library, corresponding to highly representative minerals in the Cuprite mining district, are used in this work to substantiate endmember signature purity.

Table 2 tabulates the spectral angle scores (in degrees) obtained after comparing the USGS library spectra of *alunite*, *buddingtonite*, *calcite*, *kaolinite* and *muscovite*, with the corresponding endmembers extracted by different algorithms from the AVIRIS Cuprite scene. As in the case of synthetic image experiments, the input parameters of the different algorithms have been carefully optimized so that the best performance for each method is reported in Table 2. For reference, the mean spectral angle values across all five USGS signatures is also reported in Table 2. The number of endmembers to be extracted was set to 19 in all experiments after the

[3] http://speclab.cr.usgs.gov/spectral-lib.htm

[4] http://aviris.jpl.nasa.gov/html/aviris.freedata.html

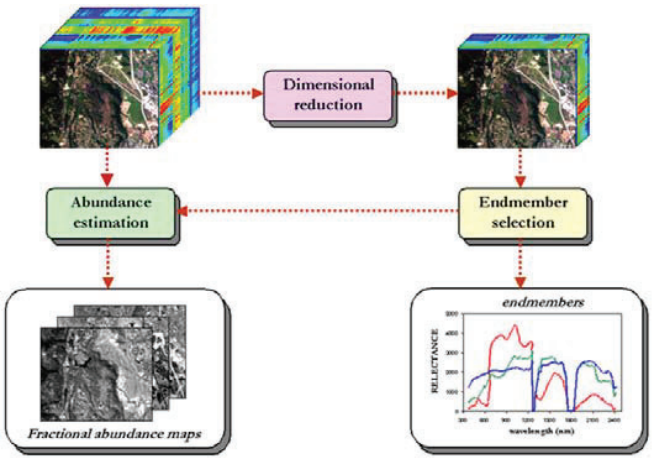

Fig. 1. Standard hyperspectral unmixing chain.

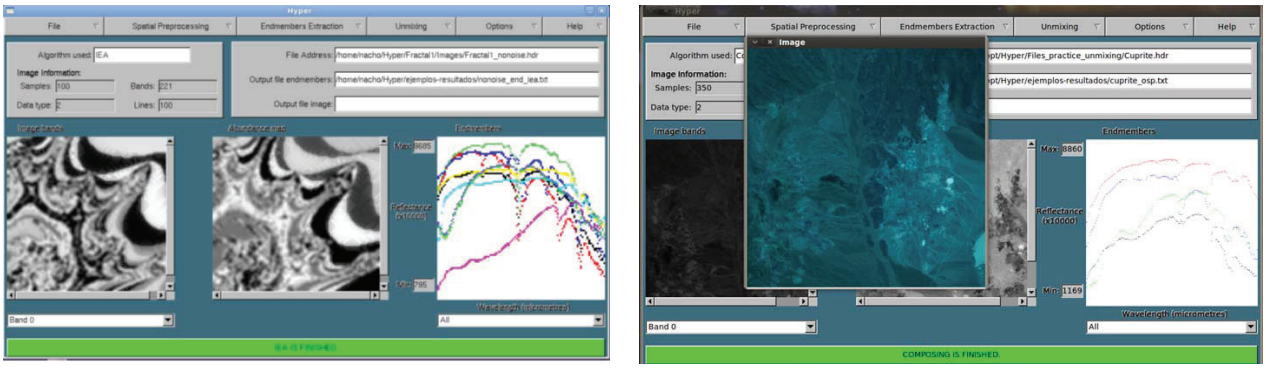

(a) Using HyperMix with synthetic data (b) Using HyperMix with real data

Fig. 2. Visual interface of the HyperMix open source tool for spectral unmixing of hyperspectral data.

consensus reached between the virtual dimensionality [18] and the hyperspectral signal identification by minimum error (HySime) [19] concepts. As shown by Table 2, the use of SSPP improved the quality of the endmembers provided by endmember selection algorithms such as VCA. In this experiment, however, the best performance (in terms of spectral angle) was obtained by algorithms including both spatial and spectral information simultaneously, such as the AMEE or SSEE.

To conclude this paper, we emphasize that further developments should be conducted in order to improve our proposed HyperMix system. In addition to the inclusion of additional techniques for endmember selection, we plan to incorporate techniques for automatic estimation of the number of endmembers in hyperspectral data such as VD and HySime. Further, we are planning to include efficient implementations that can take advantage of high performance computing systems, such as commodity graphics processing units (GPUs), to accelerate the techniques currently available in HyperMix.

5. REFERENCES

[1] A. F. H. Goetz, G. Vane, J. E. Solomon, and B. N. Rock, "Imaging spectrometry for Earth remote sensing," *Science*, vol. 228, pp. 1147–1153, 1985.

[2] R. O. Green, M. L. Eastwood, C. M. Sarture, T. G. Chrien, M. Aronsson, B. J. Chippendale, J. A. Faust, B. E. Pavri, C. J. Chovit, M. Solis, et al., "Imaging spectroscopy and the airborne visible/infrared imaging spectrometer (AVIRIS)," *Remote Sensing of Environment*, vol. 65, no. 3, pp. 227–248, 1998.

[3] N. Keshava and J. F. Mustard, "Spectral unmixing," *IEEE Signal Processing Magazine*, vol. 19, no. 1, pp. 44–57, 2002.

[4] A. Plaza, Q. Du, J. Bioucas-Dias, X. Jia, and F. Kruse, "Foreword to the special issue on spectral unmixing of remotely sensed data," *IEEE Transactions on Geoscience and Remote Sensing*, vol. 49, no. 11, pp. 4103–4110, 2011.

[5] M. Parente and A. Plaza, "Survey of geometric and statistical unmixing algorithms for hyperspectral images," *Proceedings of the 2nd IEEE Workshop on Hyperspectral Image and Signal*

Table 1. Average spectral angle scores (in degrees) between the USGS mineral spectra and their corresponding endmembers produced by several endmember selection algorithms available in HyperMix.

Algorithm	SNR=30:1	SNR=50:1	SNR=70:1	SNR=90:1	SNR=110:1
N-FINDR	2.095	0.463	0.383	0.388	0.361
OSP	2.118	0.452	0.349	0.361	0.345
VCA	1.193	0.467	0.377	0.430	0.426
SPP+N-FINDR	2.293	0.778	0.701	0.694	0.693
SPP+OSP	2.342	0.622	0.536	0.529	0.529
SPP+VCA	2.271	0.455	0.327	0.319	0.347
AMEE	2.670	1.260	0.969	1.193	1.252
SSEE	2.124	1.077	0.576	0.722	0.645

Table 2. Spectral angle scores (in degrees) between USGS mineral spectra and their corresponding endmembers produced by several endmember selection algorithms available in HyperMix.

Algorithm	Alunite GDS84	Buddingtonite GDS85	Calcite WS272	Kaolinite KGa-1	Muscovite GDS107	Mean
N-FINDR	4.81	4.29	7.60	9.92	5.05	6.33
OSP	4.81	4.16	9.52	10.76	5.29	6.91
VCA	6.91	5.38	9.53	9.65	6.47	7.59
SPP+N-FINDR	7.72	4.27	9.34	11.26	5.69	7.66
SPP+OSP	6.06	4.27	8.43	12.28	4.64	7.14
SPP+VCA	14.11	8.49	11.94	13.86	5.61	10.80
AMEE	4.81	4.17	5.87	8.74	4.61	5.64
SSEE	4.81	4.16	8.48	10.73	4.63	6.57

Processing: Evolution in Remote Sensing (WHISPERS), pp. 1–4, Reykjavik, Iceland, Jun. 14-16, 2010.

[6] J. M. Bioucas-Dias and A. Plaza, "Hyperspectral unmixing: geometrical, statistical, and sparse regression-based approaches," *Proceedings of SPIE, Image and Signal Processing for Remote Sensing XVI*, vol. 7830, pp. 1–15, Toulouse, France, Sept. 20-23, 2010.

[7] J. A. Richards and X. Jia, *Remote Sensing Digital Image Analysis: An Introduction*, Springer, 2006.

[8] M. E. Winter, "N-FINDR: an algorithm for fast autonomous spectral end-member determination in hyperspectral data," *Proc. SPIE Image Spectrometry V*, vol. 3753, pp. 266–277, 2003.

[9] J. C. Harsanyi and C.-I Chang, "Hyperspectral image classification and dimensionality reduction: An orthogonal subspace projection," *IEEE Transactions on Geoscience and Remote Sensing*, vol. 32, no. 4, pp. 779–785, 1994.

[10] J. M. P. Nascimento and J. M. Bioucas-Dias, "Vertex component analysis: A fast algorithm to unmix hyperspectral data," *IEEE Transactions on Geoscience and Remote Sensing*, vol. 43, no. 4, pp. 898–910, 2005.

[11] A. Plaza, P. Martinez, R. Perez, and J. Plaza, "Spatial/spectral endmember extraction by multidimensional morphological operations," *IEEE Transactions on Geoscience and Remote Sensing*, vol. 40, no. 9, pp. 2025–2041, 2002.

[12] D. M. Rogge, B. Rivard, J. Zhang, A. Sanchez, J. Harris, and J. Feng, "Integration of spatial–spectral information for the improved extraction of endmembers," *Remote Sensing of Environment*, vol. 110, no. 3, pp. 287–303, 2007.

[13] M. Zortea and A. Plaza, "Spatial preprocessing for endmember extraction," *IEEE Transactions on Geoscience and Remote Sensing*, vol. 47, pp. 2679–2693, 2009.

[14] C.-I Chang and D. Heinz, "Constrained subpixel target detection for remotely sensed imagery," *IEEE Transactions on Geoscience and Remote Sensing*, vol. 38, pp. 1144–1159, 2000.

[15] D. Heinz and C.-I Chang, "Fully constrained least squares linear mixture analysis for material quantification in hyperspectral imagery," *IEEE Transactions on Geoscience and Remote Sensing*, vol. 39, pp. 529–545, 2001.

[16] J. A. Hartigan and M. A. Wong, "Algorithm as 136: A k-means clustering algorithm," *Journal of the Royal Statistical Society, Series C (Applied Statistics)*, vol. 28, pp. 100–108, 1979.

[17] G. Swayze, R. N. Clark, F. Kruse, S. Sutley, and A. Gallagher, "Ground-truthing AVIRIS mineral mapping at Cuprite, Nevada," *Proc. JPL Airborne Earth Science Workshop*, pp. 47–49, 1992.

[18] C.-I Chang and Q. Du, "Estimation of number of spectrally distinct signal sources in hyperspectral imagery," *IEEE Transactions on Geoscience and Remote Sensing*, vol. 42, no. 3, pp. 608–619, 2004.

[19] J. M. Bioucas-Dias and J. M. P. Nascimento, "Hyperspectral subspace identification," *IEEE Transactions on Geoscience and Remote Sensing*, vol. 46, no. 8, pp. 2435–2445, 2008.